Ref: CERN/SPSC 2000-015,SPSC/M648 Date: March 9, 2000

MEMORANDUM

From/De : Mayda M. Velasco/Northwestern Univ., Erik Uggerhøk/ISA-Aarhus

To/à : K. Koenigsman/SPSC chairman

Subject/Sujet : Progress report on the NA59 experiment 1999 data analysis

---

The purpose of the NA59 experiment[1] is to study the use of a crystal as a 'quarter-wave plate' ($\lambda/4-$plate)[2] for polarized photons with energies above 50 GeV. This will be tested using a linearly polarized photon beam and turning a fraction of its polarization into circular.

The NA59 collaboration took data for three weeks during the 1999 SPS fixed target run with a 180 GeV electron beam, and a linearly polarized photon beam was produced from it using a carefully aligned Si-crystal radiator (See Fig. 1). Data to measure the polarization with two independent methods were taken. We had two days for the linear polarization measurement with the model-dependent 'pair' method, and eleven days with the model-independent 'ρ^0' method. The reason for the two independent measurements was to validate the 'pair' method as a successful polarimetry technique, by comparing its results to both the theoretical expectations [3, 4], and the polarization measurement obtained from the angular distributions of the π^+ π^- pairs resulting from ρ^0 photo-production. In the 'pair' method we measured the cross section asymmetry of pair conversion in a crystal between the case where the linear polarization of the photon is parallel or perpendicular to a crystallographic plane of a crystal 'analyzer' [1].

The validation of the 'pair' method polarimetry allow us to measure the effect of the proposed 10 cm long $\lambda/4-$plate Si-crystal in a time efficient way (three to four weeks).

The results on the polarization measurement with the 'pair' method and its comparison with the theoretical predictions were already presented to the SPSC on December of 1999. The results are summarized in Fig. 1, where we find very good agreement with the prediction. This already give us some confidence in this new polarimetry technique and the theoretical model used.

Now we are devoting all our attention to the ρ^0 polarization measurement. The setup used to take the data is shown in Fig. 2. A total of 1.3×10^9 electrons were delivered to us. The ρ^0 were photo-produced using a Be-target. To reconstruct the ρ^0 and the $\pi^+\pi^-$ angular distributions we need:

- the direction of the incoming photon beam, which is defined by the Delay Wire Chambers (DWC) using parent electron track. The calculated resolution for the DWC, and angular distribution of the beam divergence measured from them is shown in Fig. 3. The predicted impact point at the Be-target of the incoming photon beam using these tracks in shown in Fig. 4. This track is also used in the vertex calculation.

- in the spectrometer the track momenta are determined from the Drift Chambers (DCH). A layout of the cells in the chamber is shown in Fig. 5. The obtained hit resolution is shown in Fig. 6 for the cells in the non-bending plane. For cells in the bending plane, we limit the calibration calculation to events were there is a clear $\gamma \rightarrow e^+e^-$ pair because we can use extra constraints in the reconstruction due to the fact that the two tracks lay on top of each other at the production and only open up after the deflection caused by the dipole magnet. These events are identified from the distance between the tracks in the magnet, see Fig. 7.

- additional information and further improvement in the resolution will be eventually obtained from the available data on the Si vertex detector. See Fig. 8-9.

From this detector we are able to detect and track two track events. The expected acceptance and reconstruction efficiency is shown in Fig. 10, and the assumed event topologies in the reconstruction are shown in Fig. 11. Effects on the two track trigger condition are not included in the simulation, but they are believed not to matter, see Fig. 12.

The main expected background comes from $\gamma \rightarrow e^+e^-$ pairs. We have an electromagnetic calorimeter. However, as discussed in Fig. 13, we find it to be of limited use at this stage of the analysis. Instead, we are using the track reconstruction characteristics discussed in Fig. 14 to reject that kind of events.

The ρ^0 candidates that we find at this early stage of the analysis, using only 20% of our data are shown in Fig. 15.

At the moment, we have developed the primary tools needed to finalize this analysis and understand the resolution of our detector to a level where we can expect to do the polarization measurement to better than 5%.

References

[1] NA59 Collaboration, CERN/SPSC 98-17, SPSC/P308, July 13, 1998.

[2] N. Cabibbo, *et. al.*, Phys. Rev. Lett. **9**, 435 (1962).

[3] V. Strakovenko, private communication.

[4] Yu. Kononets, private communication.

[5] NA59 Collaboration, CERN/SPSC 99-33, SPSC/P308 Add.1.

[6] M. Velasco, Presentation to the SPSC in December 1, 1999.

[7] N. Doble, private communication.

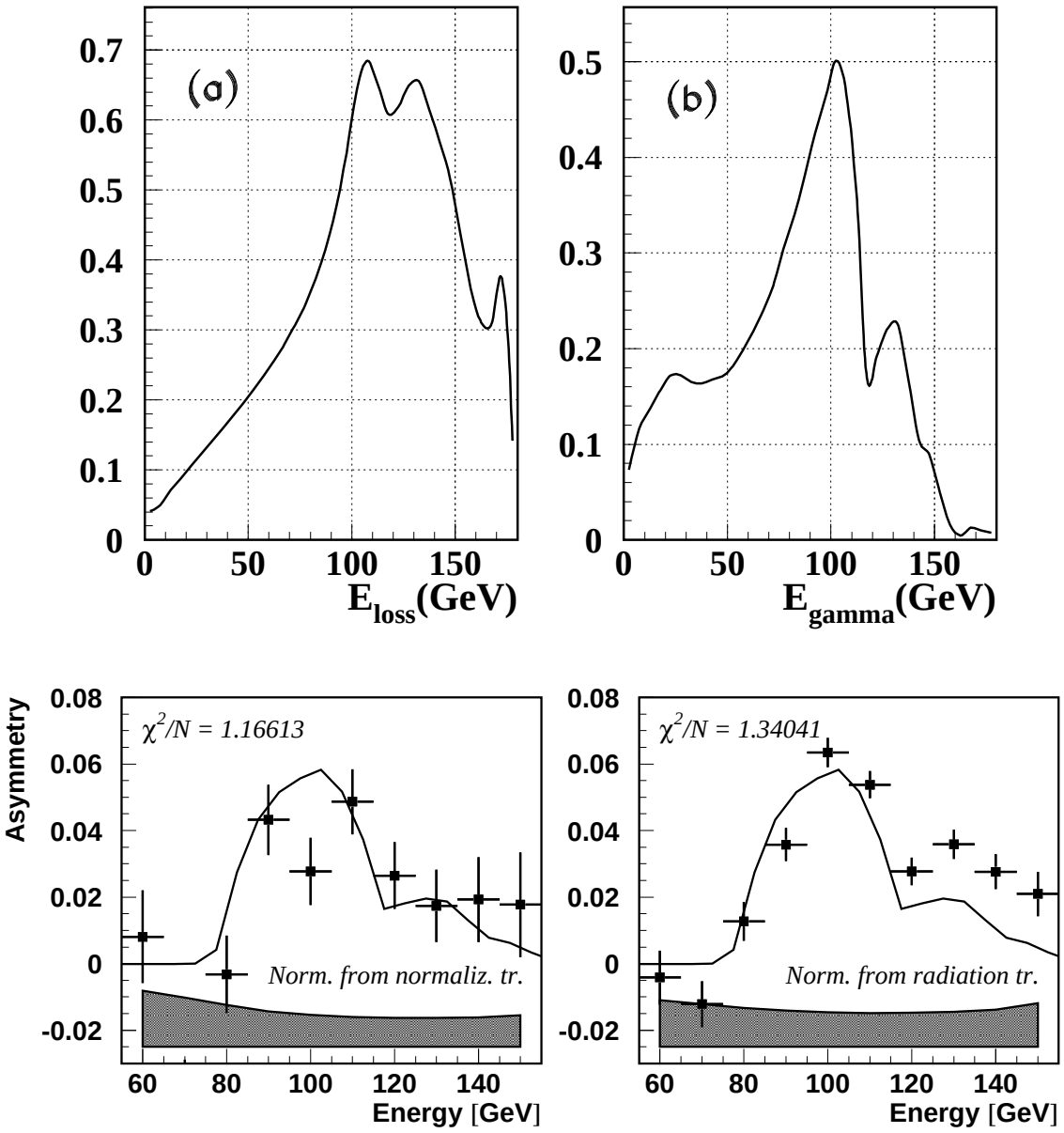

Figure 1: **SUMMARY OF RESULTS PRESENTED TO SPS IN DECEMBER**– *TOP: (a) Predictions of the relative intensity of the energy loss under the NA59 experimental condition: 180 GeV electrons penetrating a 15 mm thick Si-radiator aligned with respect to the electron beam axis at an angle of 5 mrad from the* $\langle 011 \rangle$ *axis, and 180* μ*rad from the (110) plane. (b) Expected polarization under the same conditions. BOTTOM: Asymmetry results –Evaluation of the linear polarization of the NA59 photon beam with the model-dependent method–. The asymmetry between the pair production probability,* $\gamma \rightarrow e^+e^-$*, of photons with 'parallel' and 'perpendicular' linear polarization with respect to a crystallographic plane of the impinged crystal analizer (Ge, 1 mm thick) was measured with the data taken in 1999. The two figures show the cross section asymmetry between two configurations: (1) with the analyzer's plane parallel to the expected polarization vector (corresponding to the direction of a plane in the Si crystal radiator), and (2) the data in the perpendicular configuration. The theoretical prediction shown (continuous line), to which the experimental data conforms, predicts a 50% linear polarization for the photons near 100 GeV, as shown above. The two plots differ in the choice of normalization, which, despite the difference in statistics, permit a cross check of different evaluations of trigger efficiency and acceptance.*

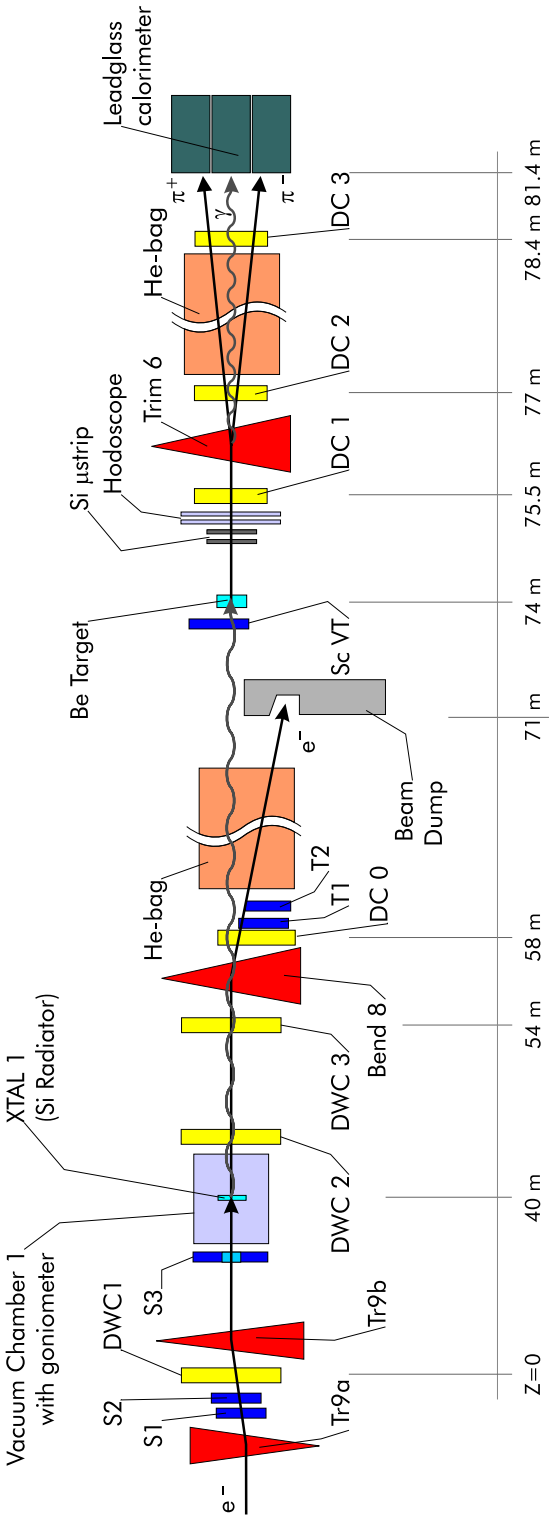

Figure 2: *Experimental setup used in the photo-production of ρ^0 used to evaluated the photon polarization in a model independent way. The main detectors discussed in the text are the DWC used to defined the electron/photon beam trajectory, DCH used in the spectrometer, and Si µstrip vertex detector.*

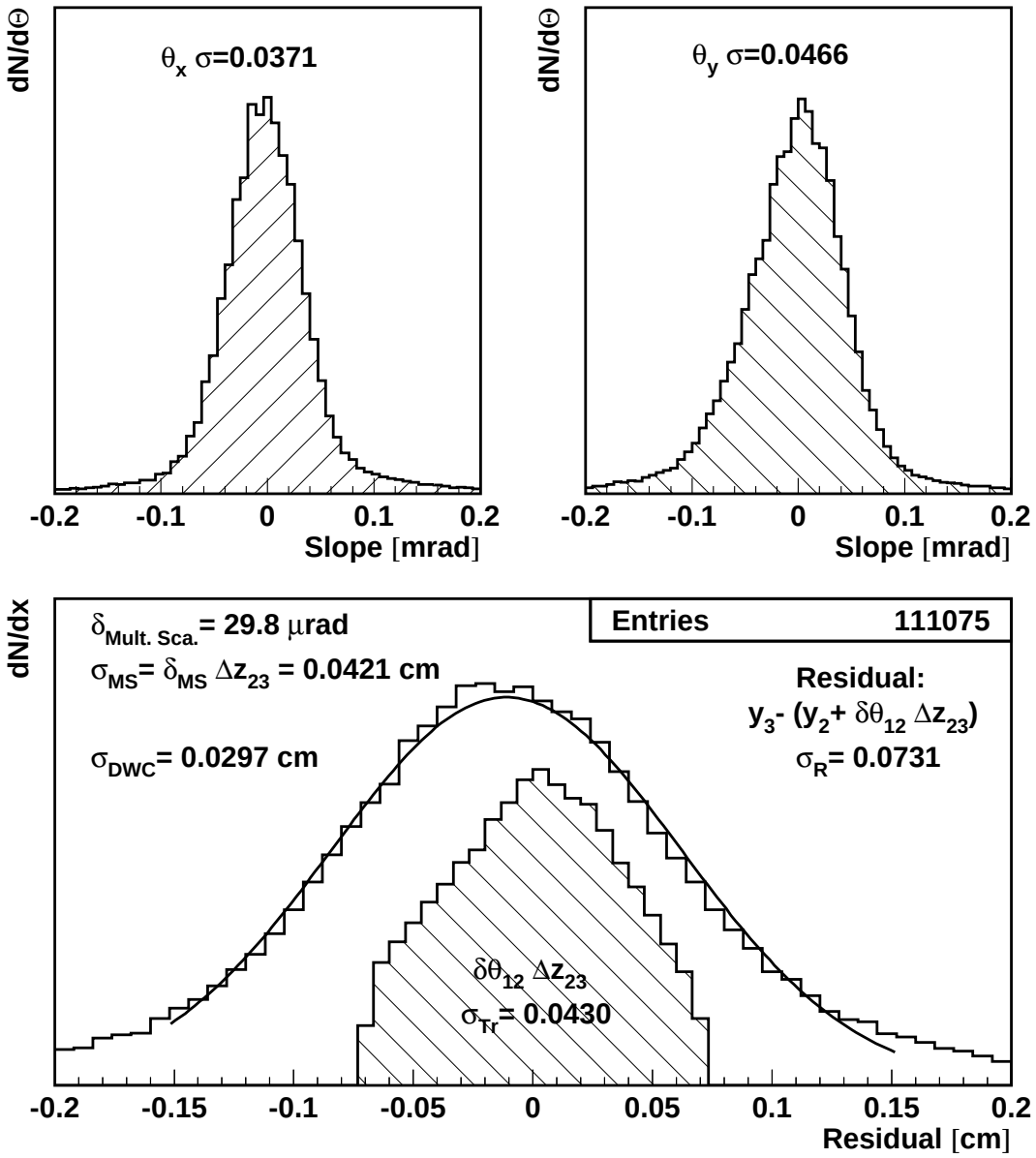

Figure 3: *The slopes in the horizontal and the vertical plane, θ_x and θ_y, are calculated from hit positions in DWC 1 and 2, and found the beam divergance to be of the order of 45μrad as expected. The resolution of the chambers, $\sigma_{\rm DWC}$ 1 and 2, is calculated from the residual of tracks from DWC 1 and 2, projected to DWC 3, and the actual hit position in DWC 3, after taking into account the multiple scattering which is mostly due to the Si crystal radiator. We define $\sigma^2_{\rm DWC} = \sigma^2_{\rm R} - \sigma^2_{\rm Tr} - \sigma^2_{\rm MS}$ where: (1)the track extrapolation resolution $\sigma_{\rm Tr}$ is the σ of the distribution of $y_{\rm Tr} = \delta\theta_{12}\Delta z_{23}$, where $\delta\theta_{12} = \frac{y_2 - y_1}{\Delta_{12}}$ is the slope from DWC; (2) $\sigma_{\rm MS}$ is the width of the expected Gaussian distribution of the angles acquired due to multiple scattering. (3) $\sigma_{\rm R}$ is the σ of the distribution of the residual $y_R = y_3 - (y_2 + \delta\theta_{12}\Delta z_{23})$.*

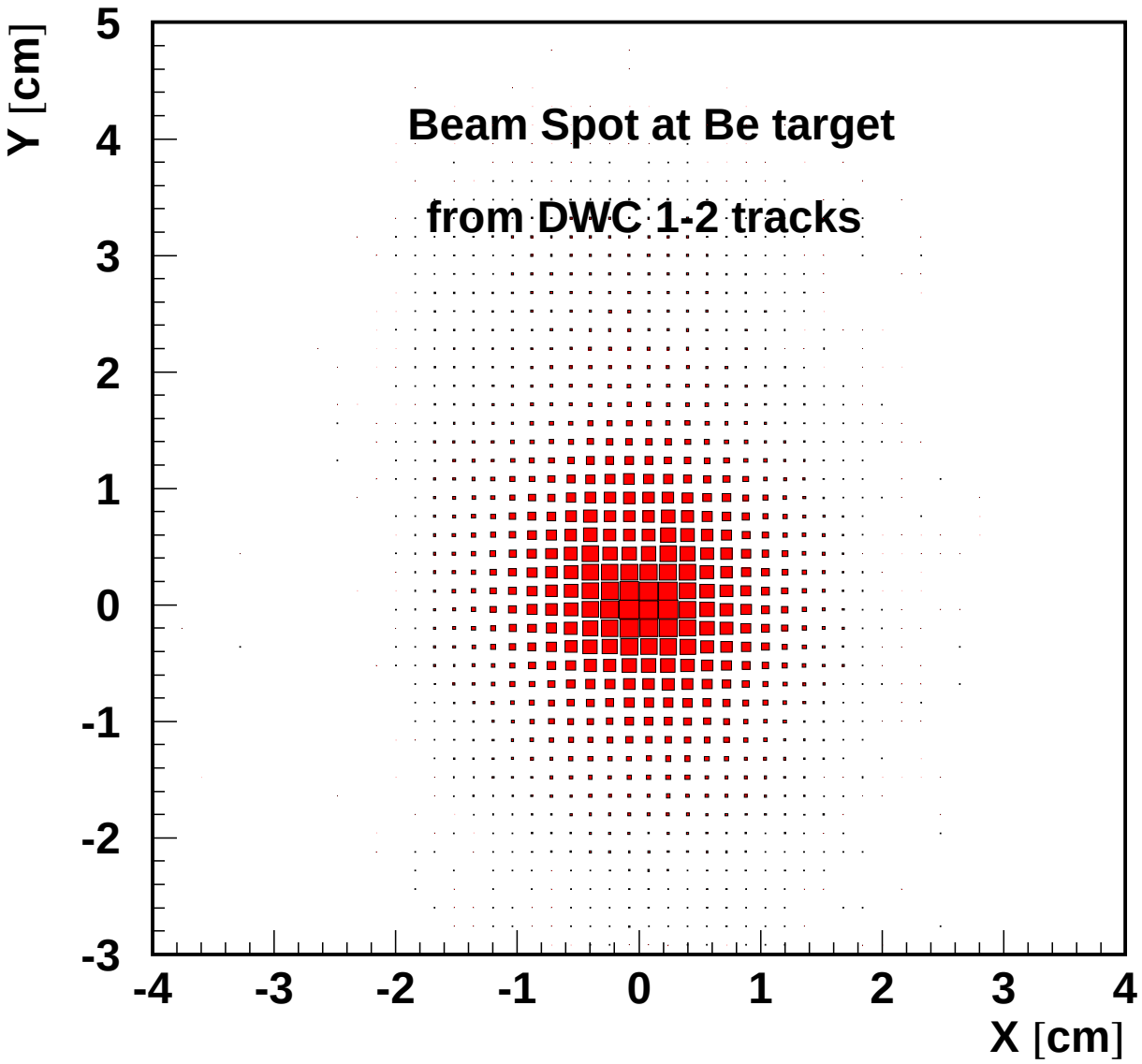

Figure 4: *Expected γ-beam spot at the Be-target measured from the electron beam track measured in the DWC 1 and 2. The diameter of the beam spot is defined by the beam collimation setings, not by the transverse size of the target. The Be-target was 6 cm long and with a diameter of 5 cm.*

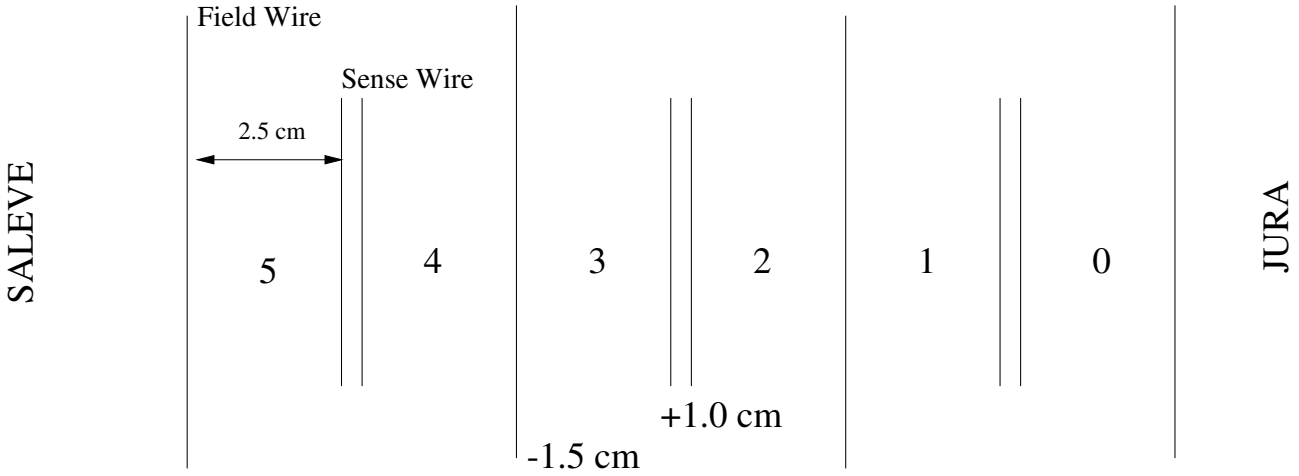

Figure 5: *Layout of the drift cells on the drift chambers used. Each plane has six cell that are 2.5 cm wide.*

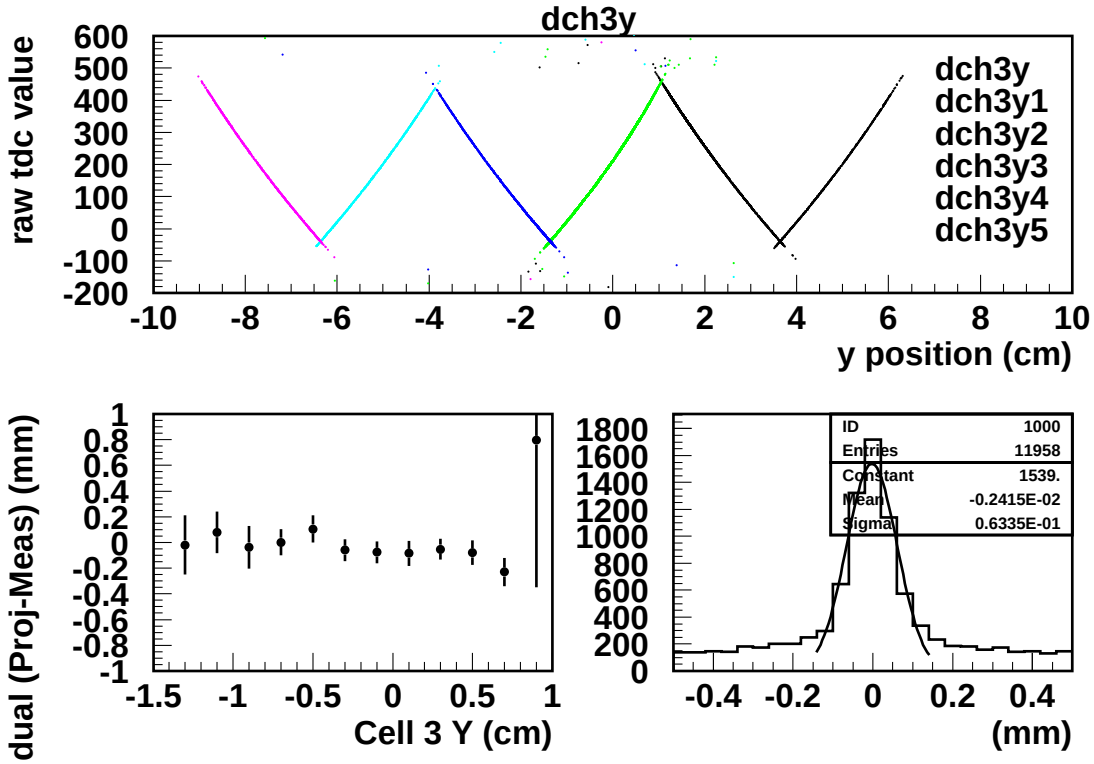

Figure 6: *Checks of the drift chamber calibration in the non-bending plane of the spectrometer using 'physics' data rather than low intensity calibration data. On TOP we show the correlation between extrapolated tracks to DCHY3 which were reconstructed from DCHY1 and DCHY2 hits and the raw TDC values recorded in DCHY3. The plot shows the expected drift direction described in Fig. 5 and the TDC counts are consistent with the range in drift time. Plots in the bottom show the uniformity of the resolution of the chamber within a cell and the overall chamber resolution, which is expected to be better than 100 μm.*

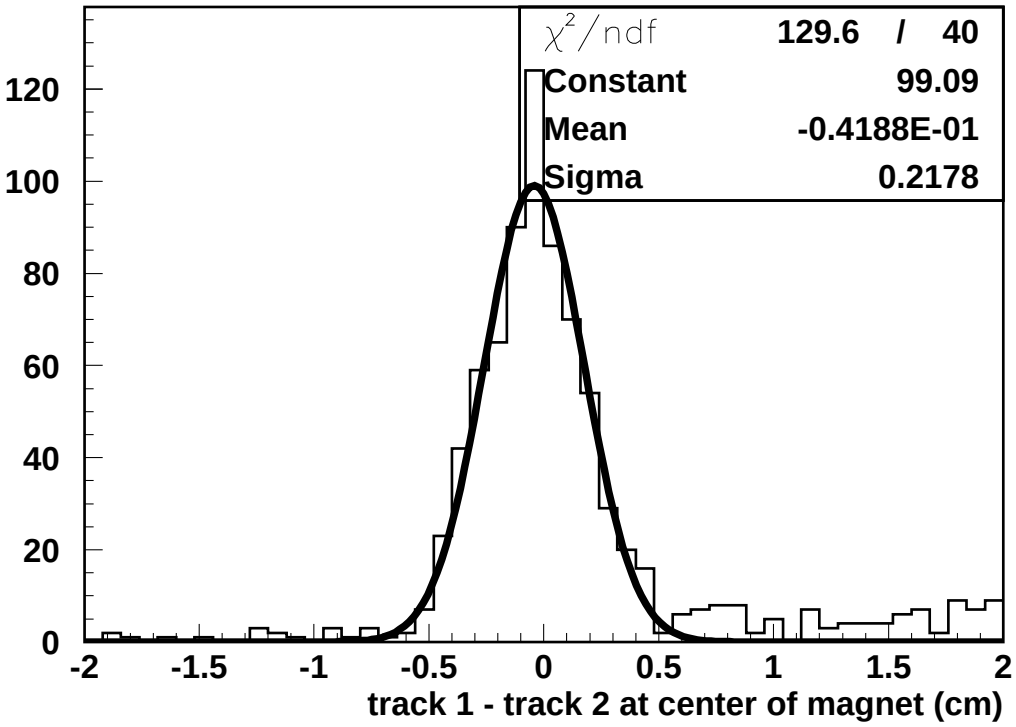

Figure 7: *Checks of drift chamber calibration using 'pair-physics' data in the bending plane of the spectrometer. We use $\gamma \rightarrow e^+e^-$ events because there is no opening angle between the e^+e^- pair and the can be easily identify as Y-looking type of events, and use the magnet position as an extra constraint. Therefore we can assume that upstream of the magnet there is only one track, while the downstream tracks should approximately meet at the center of the magnet. Hit position resolution of about 100 μm was found, just like the cell in the non-bending plane. The same event topology identification is used to reject $\gamma \rightarrow e^+e^-$ data in the ρ^0 sample as shown in more deteiled in Fig. 14.*

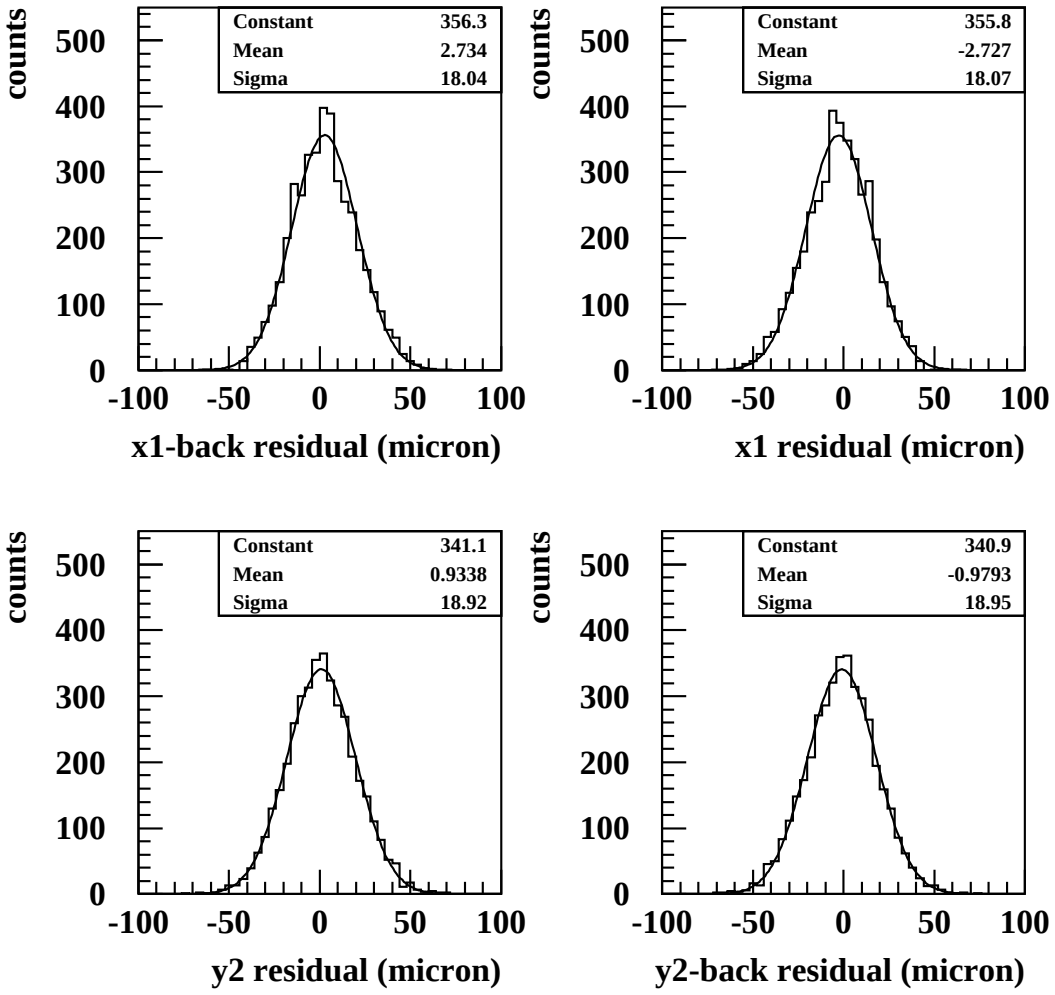

Figure 8: *Plane resolution of Si μstrip detector is $\sim 20\mu m$. They will be used to improve the reconstruction of events already identify as 'ρ^0' candidates.*

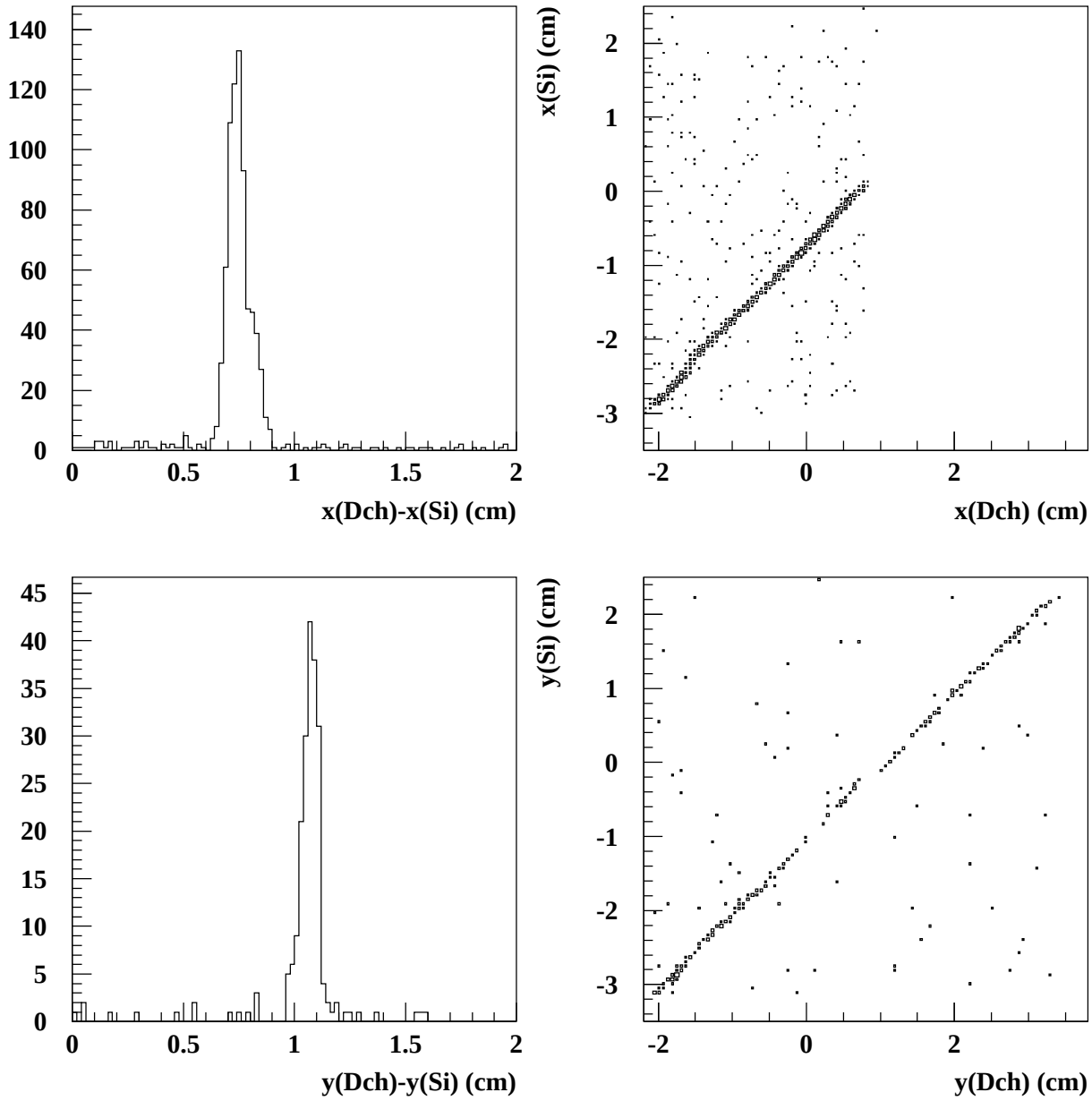

Figure 9: *First look at the correlation between hits in Si μstrip detector and the first drift chamber DCH1. The alingment with respect to the rest of the spectrometer will now be done, and the Si μstrip detector information will be added to the reconstruction. Note: one cell in the x-view was disconnected during this test run data.*

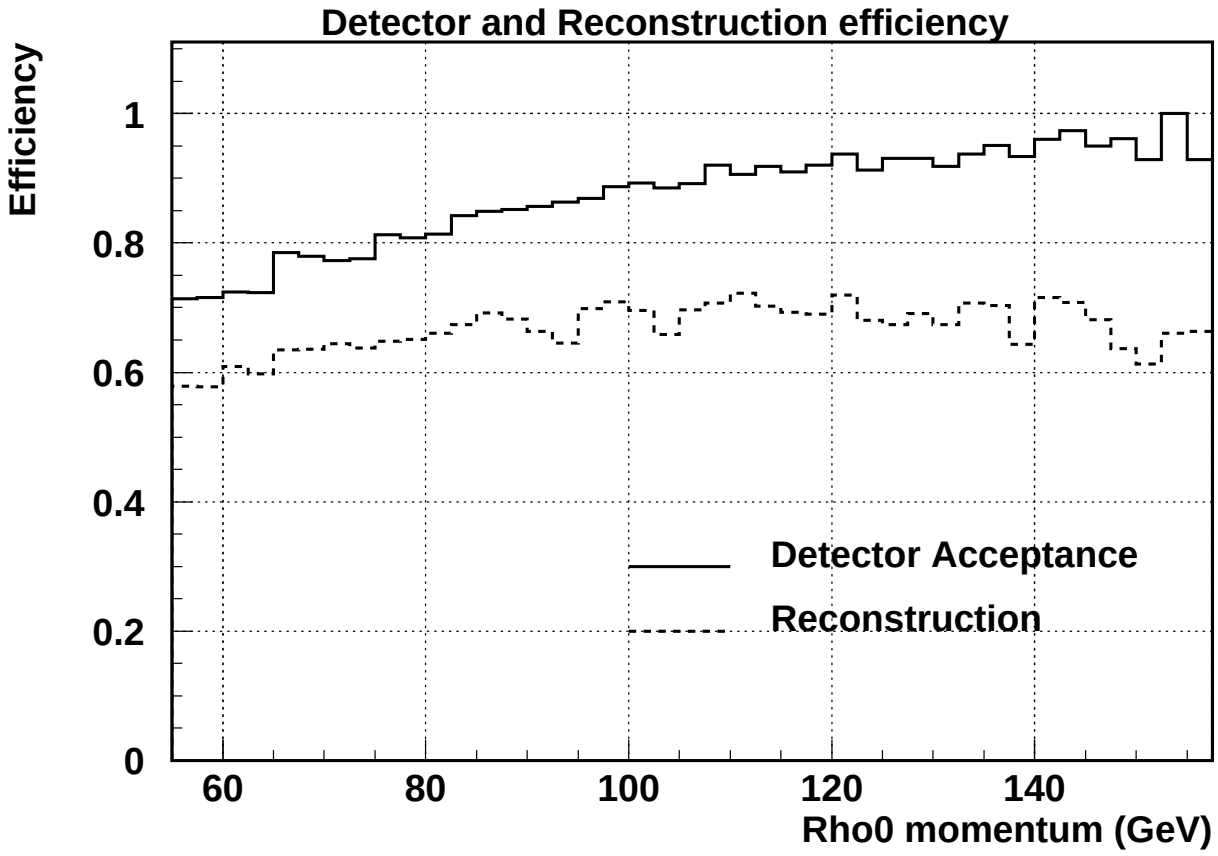

Figure 10: *Acceptance of ρ^0 in our detector and expected reconstruction efficiency.*

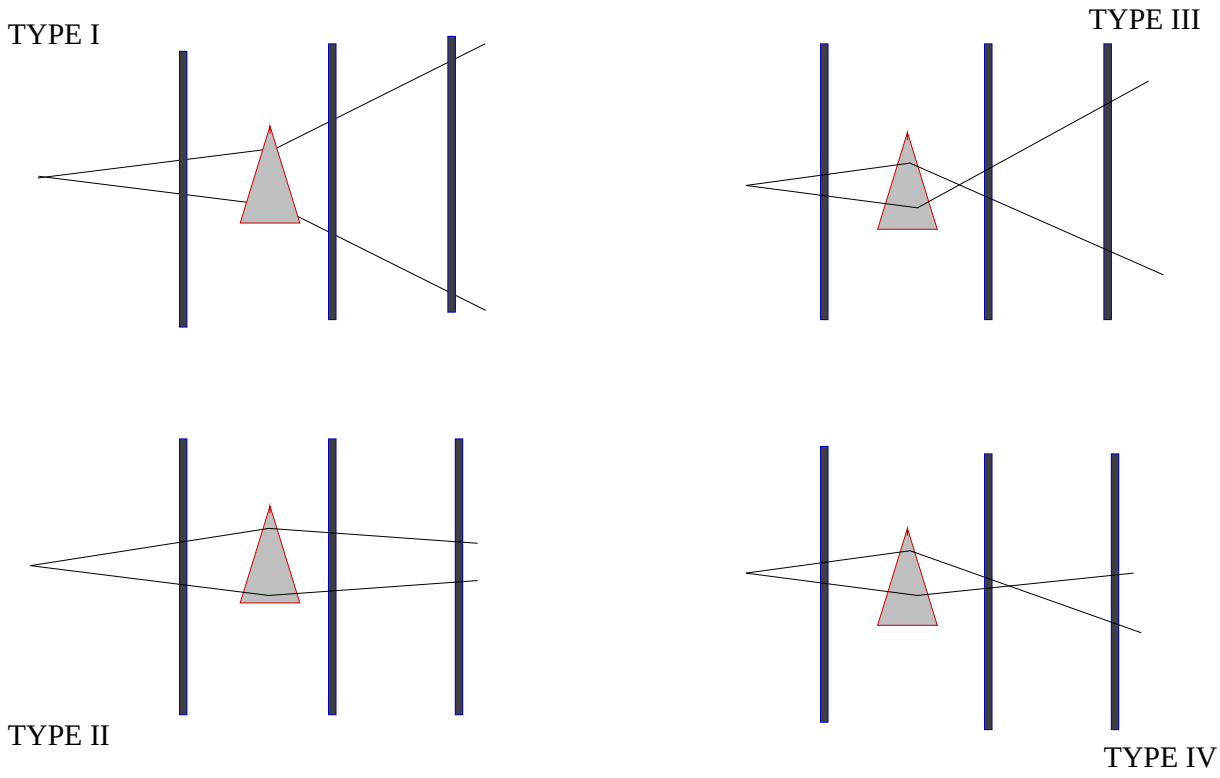

Figure 11: *Event types: we find that more that of the 60% of the recostructed events are TYPE1, while given the strenght of our magnet, we should not have TYPE3-4 for ρ^0s with more that 50 GeV. This fact is used as cross checks in the validity of the reconstructed track.*

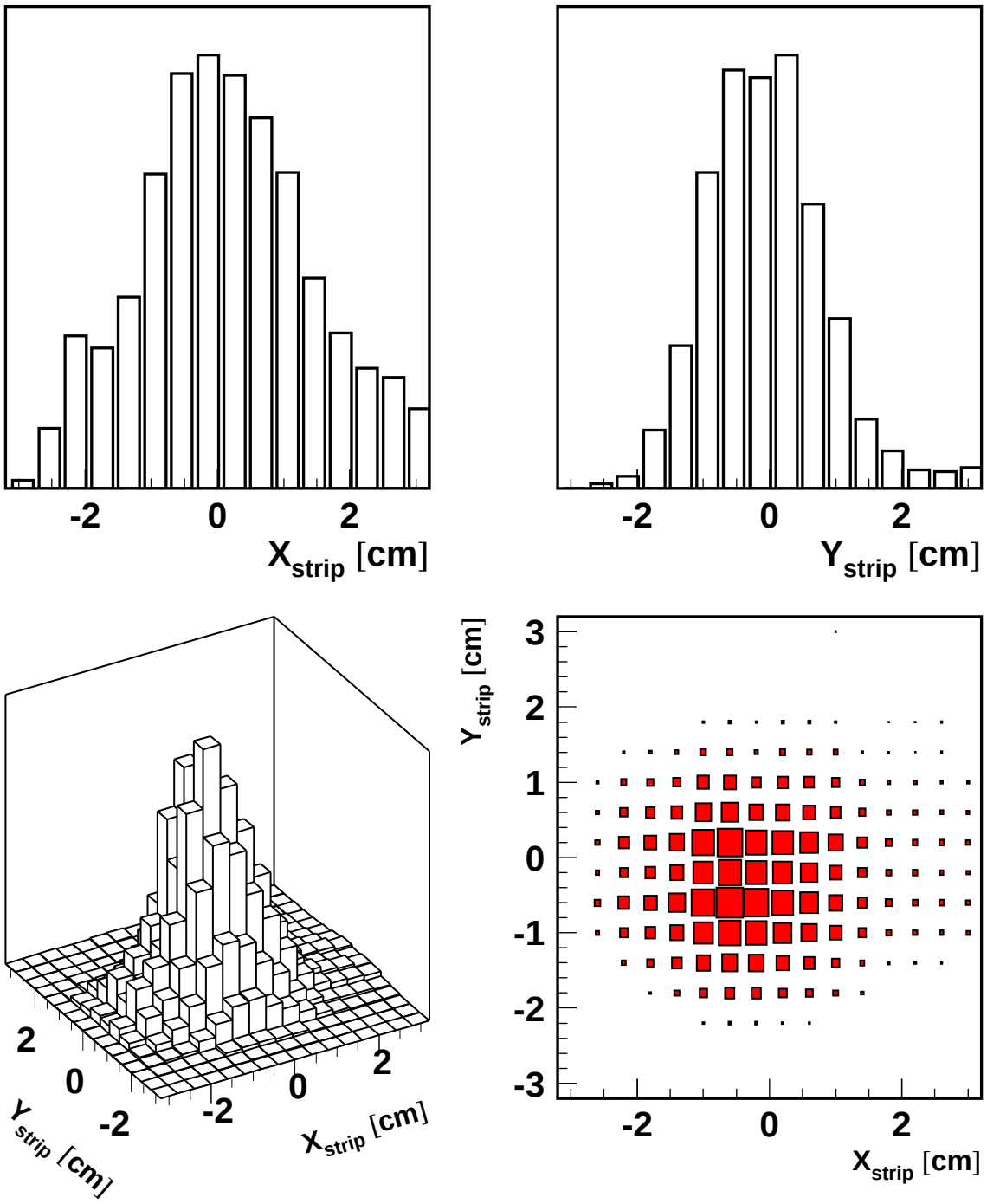

Figure 12: *The two-track trigger used in the ρ^0 analysis required two hits in either the horizontal or vertical plane of the hodoscopes, and it had the 'radiation' trigger as a pretrigger. The efficiency and acceptance of the radiation trigger was already discussed in [5, 6]. The two track condition will be studied next. We don't expect any correction to be needed since the hodoscopes have been found to be very stable during the whole data taking, and the requirements to construct the signal are not strong.*

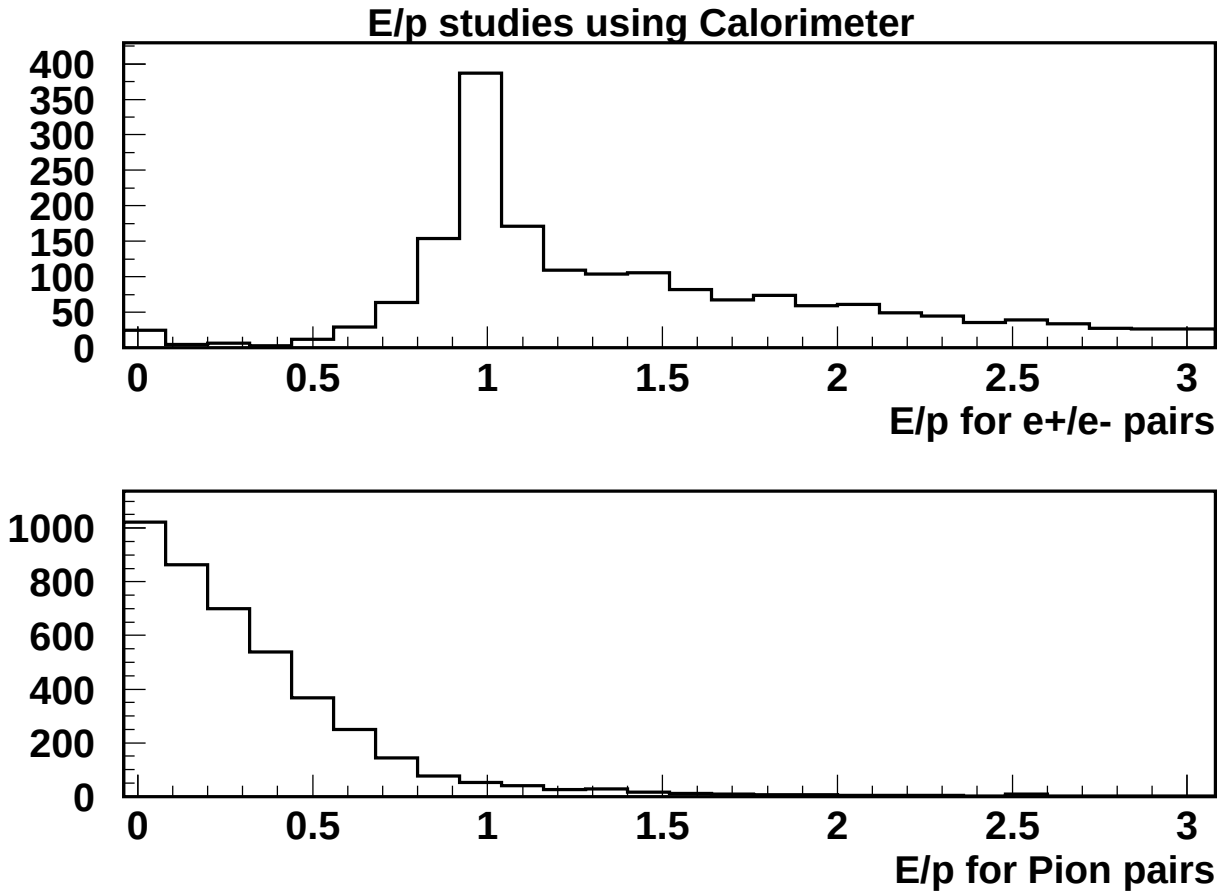

Figure 13: *The lead glass calorimeter is made out of blocks that have a cross sections of 9×9 cm. From MC studies we can see that in the case of $e^{\pm}$ 66% of the energy is deposited in the "entrance" cell and 34% of the energy is deposited in the neighbouring cells, similarly for pions. Therefore, even though the e/π separation should be possible, in reality the overlap between individual showers is significant and for this reason we can not make E/p cuts on individual track basis.A In addition, a signifant fraction of the tracks enter in the central cell, where we also have the energy of the uncoverted photons (the average photon multiplicity is about 3). Other methods of rejecting $\gamma \rightarrow e^+e^-$ events are discussed in Fig. 13 and Fig. 15.*

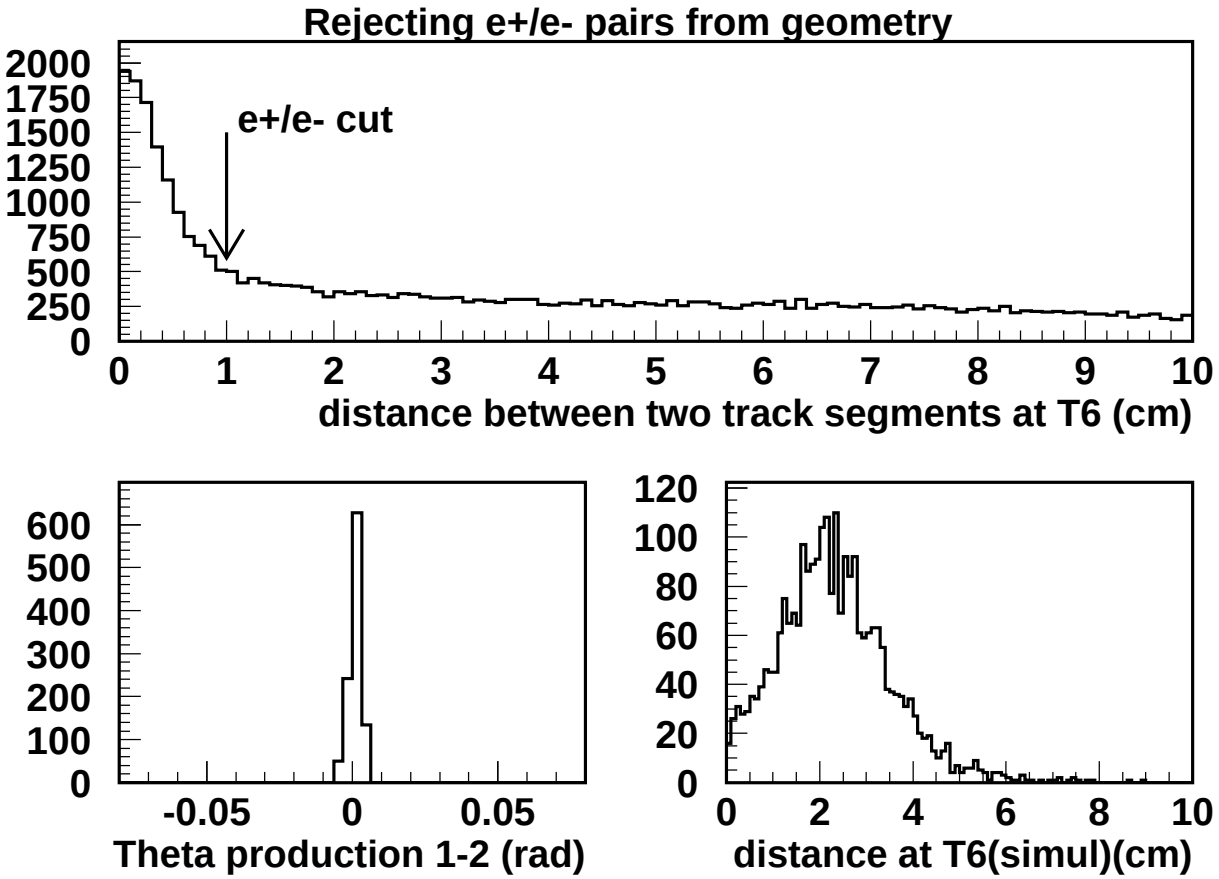

Figure 14: $\gamma \to e^+e^-$ *identification from calorimeter independent properties. The Y type events which also exist in* ρ^0 *data can be identified from the distance between the projection of two outgoing track segments back to the T6, TOP plot. BOTTOM left: Imposing a cut on this distance at 1 cm leaves events with a very small production angle, which is consistent with the zero invariant mass of the photon. Another cut on the TOP plot is from the maximum expected* P_t *that the* π*s can have if they are produced by* ρ^0*'s. Therefore events with a distance between the projection of two segments at T6 greater than 6cm are not* ρ^0 *candidates and therefore rejected.The Monte carlo simulation on which this cut was turned is shown in the BOTTOM right corner.*

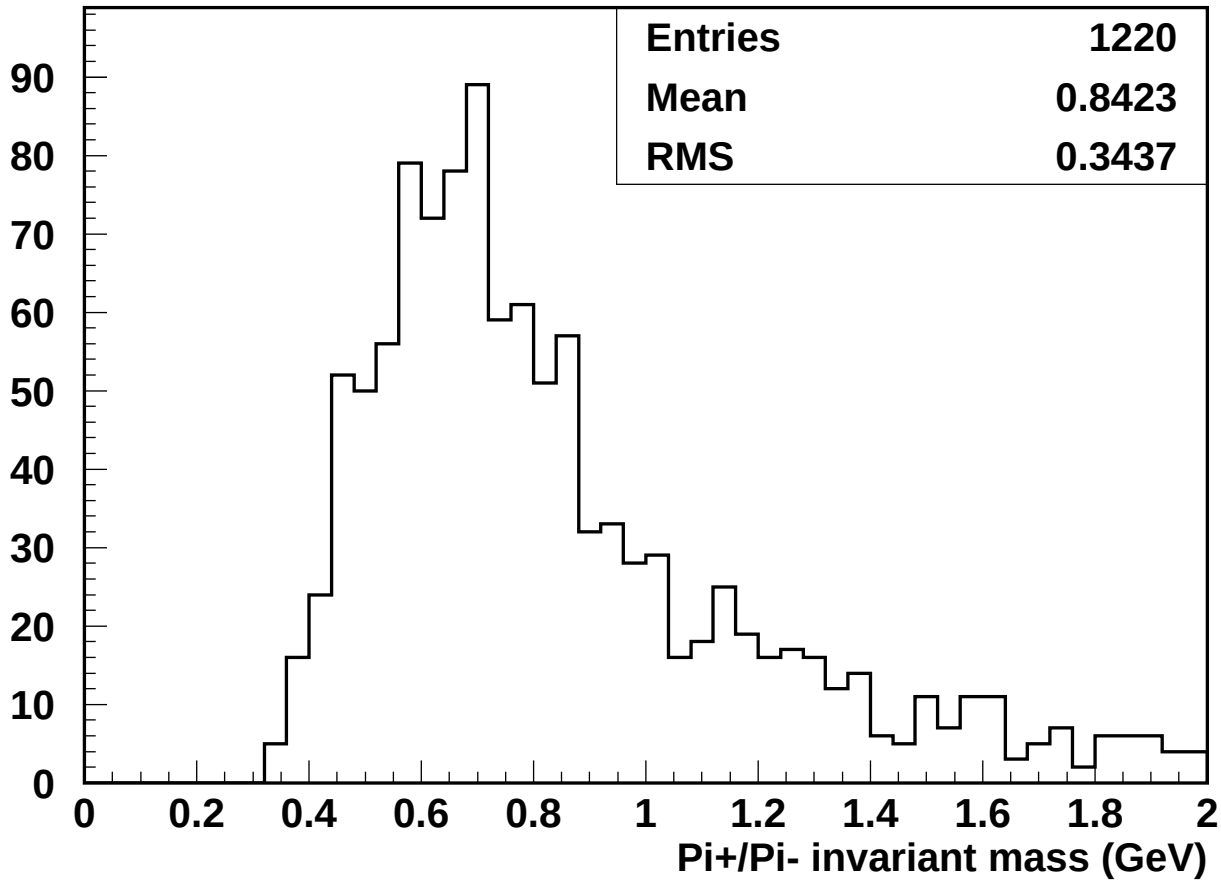

Figure 15: *Preliminary reconstructed ρ^0 candidates based on 20% of the available data. Remaining background to be reduce from the combined information on total $E/(p_1 + p_2)$ in the magnet and the electron beam energy loss measured from the upstream electron spectrometer (Bend-8).*